JOINT EUROPEAN TORUS JET

JET–P(93)103

H.P.L. de Esch, D. Stork, C. Challis, B. Tubbing

The Optimisation of Neutral Beams for Ignition and Burn Control on Next Step Reactors

The Optimisation of Neutral Beams for Ignition and Burn Control on Next Step Reactors

H.P.L. de Esch, D. Stork, C. Challis, B. Tubbing.

JET-Joint Undertaking, Culham Science Centre, OX14 3DB, Abingdon, UK

Preprint of a paper to be submitted for publication in
Fusion Engineering and Design
December 1993

ABSTRACT

The purpose of this paper is to identify the Neutral Beam Injection (NBI) parameters for a system on a Next Step reactor, optimised for ignition and burn control, rather than current drive. As a main model we use the ITER-EDA concept in its 1993 version (R_0=7.75m, I_p=25 MA, B_T=6T, a=2.8m, k=1.6). The dependence of the 'minimum power to ignite ITER-EDA' on beam energy, beam geometry and beam isotope species is investigated for a plasma, which conforms to Rebut-Lallia-Watkins transport in time dependent simulations. It is found that deuterium beams with an energy of 400 keV or above in a geometry with tangency radius (R_T) approximately half the major radius, are sufficient for efficient ignition. The beam simulation results are compared with simulations using an idealised heating scheme. Sensitivity of the results to variations in plasma behaviour are investigated. Impurities, particle confinement, energy confinement and the H-mode threshold are factors which influence the power required for ignition significantly, but have little effect on the choice of beam energy and geometry. Considerations with respect to loss of fast particles led us to adopt a beam geometry with $R_T \sim \frac{1}{2}R_0$ (very similar to that of JET), rather than perpendicular injection. Finally it will be shown that burn control using NBI is possible on ITER-EDA in sub-ignited regimes.

1. INTRODUCTION

Previously, optimisation of Neutral Beam Injection (NBI) for a Next Step device like ITER, has considered only current drive. The main problem with current drive of any sort is the high power required to drive a significant current in a device like ITER, which is not particularly optimised for current drive and steady state operation. As pointed out by Rebut [1], this leads to a very high recirculating power, which can be similar to the foreseen fusion power itself.

The requirement for high current drive efficiency led the ITER-CDA team [2] to propose a very tangential NBI injection angle and a high (1.3 MeV) injection energy.

The present status of the ITER engineering design activity (EDA), as presented by Rebut [3], excludes the use of such tangential neutral beams, because the ITER ports had to be narrowed to accomodate 24 toroidal field coils in stead of the 16 coils previously. In effect, with the present (October 1993) design status, Neutral

Beam current drive cannot be achieved with reasonable efficiency and it seems appropriate to investigate optimising a neutral beam system for heating, ignition and burn control.

Neutral Beams, optimised for heating and ignition, should be lower power and may yield advantages in terms of smaller size and simplification. A conceptual design for such a system is presented by Hemsworth [4]. Here, we deal with the physics considerations which led to the adoption of the parameters in Hemsworth's paper. The sensitivity of ignition to Beam energy, power, geometry, species and pulse length has been established. In addition the use of a NBI system to achieve successful burn control has been evaluated.

2. OVERVIEW AND DESCRIPTION OF THE SIMULATION PROCESS

Boucher and Rebut [5], using the predictive code PRETOR written by Boucher [6], achieve ignition in ITER-EDA (Table 1) using 10 MW of idealised heating (called "RF") into a plasma diluted with 1% beryllium. This code uses the Rebut-Lallia-Watkins (R-L-W) model [7] to predict the heat transport coefficients from the plasma parameters. The particle diffusivity coefficient is assumed to be half the electron heat diffusivity and the particle pinch velocity is calculated, using a model by Boucher [8]. The original code handles current diffusion, radiation, hot and cold neutrals and a main plasma with constant tritium and impurity fraction plus a helium species.

This code was modified to include Neutral Beams. This made it necessary to include a fast particle population. The alpha particles are treated in the same way. Because of beam particle fuelling, the modified version of the code handles H/D/T species, helium and one additional impurity, each individually consistent with the R-L-W modelling. After these changes, we were able to simulate ignition in ITER-EDA with 12 MW of idealised heating, and with 17 MW of NBI heating.

Neutral Beams are modelled by a single pencil beam. Tangency radius, vertical position at the tangent point and vertical angle can be chosen. Ionised fast particles are produced along the pencil according to the most recent multistep ionisation cross-sections [9] and are assumed to remain on the birth flux surface and follow Stix [10] slowing down in losing their energy. The beam model has multiple isotopes and beam-energies. Once slowed down, the beam particles are

added to the main plasma. The alpha particle fusion products follow the same Stix modelling. Once they are slowed down, they are added to the helium impurity species.

Throughout this paper, we assume that 1% of the particle flux coming out of the plasma is pumped, which is the same assumption as Rebut and Boucher [1,5] make. However, larger beryllium impurity fractions than 1% will be considered.

To understand the methods used in these studies, consider first a plasma with density n and temperature T. The additional heating power to maintain such a plasma (ie, ensure $\partial T/\partial t=0$) can be calculated from the radiated and the conducted power if the confinement time is known. In this way, additional heating contours in (n,T) space can be calculated. Fig. 1 gives such a plot (calculated by the POPCON code, Uckan [11]) for the ITER-EDA device and an R-L-W confinement time. Note that Ohmic power and alpha particle power are excluded from the additional heating.

Fig. 1 shows a general feature of these simulations. If a low density plasma is heated, ignition is never achieved. If a high density plasma is heated, ignition can only be achieved at the expense of high additional power. An optimum route to ignition is obtained by starting at low density and ramping the density as heating is applied, so that the plasma passes through the saddle point in Fig. 1. The saddle point has become known in the literature as the 'Cordey pass'. Once the plasma is on the high temperature side of the Cordey pass, the excess additional power needed to get through the pass will push the plasma into the ignition zone.

In the code, the Cordey pass was found by starting the simulated plasma at low density, then applying heating power and ramping up the density. By varying the heating power on successive runs, the value to surmount the Cordey pass was found. This 'Minimum Power to Ignite' was then studied to highlight its dependence on parameters associated with the NBI system.

3. RESULTS OF IGNITION STUDIES: NEUTRAL BEAM SYSTEM PARAMETERS

All studies in this section have been done for an ITER-EDA D-T plasma, contaminated with 5% Beryllium, which is less optimistic than the 1% Rebut *et al.* [5] assume. The transport model is the Rebut-Lallia-Watkins [7] model. In all simulations, the density is ramped slowly (in 195 seconds) from 5.10^{19} to

16.10^{19} m^{-3}. Mono-energetic D^o beams (as would be derived from a negative ion system) are assumed, unless stated otherwise. The effect of different assumptions to those stated above will be discussed in section 5.

3.1 Minimum Power to Ignite ITER: Beam Energy and Tangency Radius dependence

Fig. 2 shows the variation of the minimum NBI power required to ignite ITER-EDA as a function of the D^o beam energy. The results shown are for a beam tangency radius of 4m. This corresponds to an achievable value of R_T given the present ITER-EDA port design [12], which allows a beam geometry very similar to that of JET (Thompson [13]). The figure shows that the power required is a slowly varying function of the beam energy $E(D^o)$ until one reaches the regime $E(D^o) <$ 400 keV. Part of the very steep variation at energies below 200 keV is caused by the upset of the D:T ratio in the plasma due to beam fuelling (see sect 3.3).

In order to quantify the systematics of NBI heating, the concept of the 'Threshold energy' is introduced. This is the beam energy at which ignition occurs with a power 50% higher than the power at the optimum beam energy. The variation of this threshold energy with beam tangency radius is shown in Fig. 3, where it can be seen that the more tangential beams will require higher energies to ignite the plasma.

3.2 Systematics of NBI heating.

The code runs show the variation of the ion heating capability of an ignition NBI system. In Fig. 4, the NBI power coupled to the plasma ions is shown as a function of D^o beam energy. The data is evaluated just before the plasma ignites. It can be seen that D^o beams do not predominantly heat the plasma ions, unless the beam energy is below 300 keV. In the central 20% volume of the plasma, however, ion heating dominates below 750 keV. It is thus clear that the NBI systems on ITER-EDA will have a different effect on the plasma from the present generation positive ion systems, which are predominantly ion heaters.

The power fraction (relative to total NBI power) which is given by beam-plasma fusion reactions is also plotted in Fig. 4. It can be seen that an increase of less than 10% of the NBI power comes from the inclusion of the beam-plasma power.

The balance between central and peripheral NBI heating is shown as a function of D^0 beam energy (again just prior to ignition) in Fig. 5. It can be seen that penetration increases with beam energy, but above 1 MeV shinethrough starts to limit the advantage for a tangency radius of ~4m. As discussed below, the penetration advantage does not translate into a large advantage in ignition capability.

3.2.1 Peripheral vs. central NBI heating

An examination of the time dependence of the heating profiles is revealing in explaining why there is only a slowly-growing advantage of beam penetration. Figs 6(a) and 6(b) compare heating profile evolution for medium energy (600 keV D^0) and low energy (250 keV D^0) cases. It can be seen that although the NBI heating profile is more peripheral in the 250 keV case, the profile of the α-particles produced rapidly becomes dominant. After 55 seconds, the α-power is dominant in both cases, and the time history is one of α-particle, rather than NBI, heating. This dominance by the α's, which are overwhelmingly electron heaters, leads us to expect that the advantages of an additional ion heater system will be limited for igniting a plasma (see sect. 4.1).

3.3 Effects of mixed D^0/T^0 beams and H^0 beams

The results displayed so far concern the injection of pure D^0 beams into a plasma with an initial 50:50 D/T mix. As a result of this excess D^0 fuelling, the balance of deuterium and tritium in the plasma will change from the optimum ignition mix (50:50). At most of the NBI energies considered this is not a large effect; partly because the ignition product, proportional to $n_T n_D$ or $f_T(1-f_T)n_e^2$, is a slowly varying function of the tritium fraction f_T; and partly because the D^0 particle flux from high-energy beam systems is low. Only when the D^0 beam energy is lower than 200 keV, the minimum power to ignite ITER-EDA with D^0 NBI alone will be 20% or more above the requirement for mixed D^0/T^0 beams.

These results are sensitive to the particle flux at the edge (poorly known experimentally) and to the pumped fraction of particles coming out of the plasma. If, for example using 250 keV D^0 beams, the particle flux at the edge is reduced by a factor of 3, relative to the model prediction, the D/T ratio in the plasma changes from 60/40 to 70/30. The fusion power would drop 12%. This change in D/T ratio could be offset via the gas puff, but this has not been

simulated. At higher beam energy, the effects from beam fuelling are much smaller.

Hydrogen beams (H^o) have a distinctly different impact on the plasma because H particles do not constitute fuel. Simulations show that it is still possible to ignite ITER-EDA using H^o beams. The power required for ignition is around 20% higher than for D^o beams, provided the beam energy is chosen above 750 keV. Below $E(H^o)$=750 keV progressively more power is needed to ignite, and below 400 keV ignition is not possible anymore due to hydrogen poisoning of the plasma (quite similar to the helium poisoning discussed later).

3.4 Loss mechanisms for the NBI particles

3.4.1 Beam Shinethrough

The beam shinethrough onto the inner wall depends on plasma density, beam energy and beam tangency radius. For 600 keV D^o beams with a 4m tangency radius into a $n_e=4.10^{19}$ m^{-3} ITER-EDA plasma, the shinethrough is 2%. For 800 keV beams the value is 5%. This can again be reduced to 2% by injecting into a 5.10^{19} m^{-3} plasma. For 1 MeV beams the shinethrough is below 8% for $n_e \geq 4.10^{19} m^{-3}$. A realistic beam geometry would indicate that this power is spread over 0.5 m^2 or more on the tokamak inner wall. For 25 MW NBI power per beamline, this would give 5 MW/m^2 on the inner wall, so we would not expect any significant problems with any reasonable inner wall armouring (which must exist to protect the ITER-EDA inner wall from events associated with plasma movement).

If perpendicular injection were to be used on ITER, the numbers quoted for shinethrough approximately double in magnitude. The shinethrough for H^o beams is approximately 4 times as high as for D^o beams around E=800 keV and $\langle n_e \rangle = 5.10^{19}$ m^{-3}.

3.4.2 Ripple Loss for NBI particles.

Direct ripple losses depend critically on where the ripple well region is. Various ITER-EDA ripple maps (for 24 toroidal field coils) appear to be quite different. The largest region is in the TAC-3 report [3], but this particular design version was rejected by the TAC committee [18], which recommended to return to an older

design version. Hence we used maps based on older designs (with R_0=7.75m). For these designs, the ripple well region is fairly small.

Calculations have been done for 600 keV D^0 injection at various injection angles. The biggest loss of beam power was found to be the case for perpendicular injection (R_T=0): 12%. For the tangency radii of 2, 4 and 6 m, the power loss was 6%, 2.6% and 0.8%, respectively. The calculations included stochastic diffusion.

4. RESULTS OF IGNITION STUDIES: STUDIES WITH IDEALISED HEATING

An idealised heating scheme is a such that heating location, heating profile width and power fraction to the ions can be chosen at will, allowing the demonstration of physics effects. Such a scheme was used extensively by Rebut *et al.* [1,5,6]. They call it 'RF' (with the power to the ions fixed at 50%), but it does not correspond to any realistic RF scheme, and should not be used to compare NBI with RF. Rather we use it here in order to investigate systematics and see how close an NBI system is to being the ideal heater. Unless stated otherwise, the same plasmas are used as in sect. 3.

The Idealised Heating Scheme has been used to assess the beneficial effect of heating the ions. If one goes from a scheme which delivers 100% of its power to the electrons to a scheme which delivers 100% of its power to the ions, the minimum power to ignite ITER-EDA is reduced by 30%.

The effect of power deposition profile width has also been investigated. The narrower the deposition profile gets (with its peak in the plasma centre), the less power is needed to ignite. However, once the deposition width (defined as a Gaussian) becomes less than 30% of the tokamak's minor radius, there is no more advantage to be gained in making the profile narrower.

The power to ignite using NBI can be compared to the power to ignite with Idealised Heating. Fig. 7 compares the minimum power to ignite ITER-EDA for beams and Idealised Heating at different starting densities. 600 keV D^0 beams with JET-like geometry (R_T=4m) are chosen. The Idealised Heating gives 40% of its power to the ions and has a 1/e width of 2m. This profile was chosen such, that it matches the beam-power requirement at $\langle n_e \rangle = 5.10^{19}$ m^{-3}. Because the beam deposition profile depends on the density (and the idealised heating profile does not) progressively more beam power is needed at higher densities.

The Idealised Heating requirement increases too. The increase is caused by the fact that during the time development of the plasma, it no longer traverses the Cordey pass. The difference between NBI and Idealised Heating is caused by the progressively lower NBI penetration at higher density.

As mentioned, the Idealised Heating profile was chosen to match the NBI power requirement. If the profile width of the Idealised Heating is made very narrow, the minimum power to ignite ITER-EDA is reduced by 30%. Hence realistic NBI heating, at a reasonable beam energy, needs 40% more power than Idealised Heating. This ratio is found in all simulations where the beam energy is well above the threshold energy and the starting density is low.

5. RESULTS OF IGNITION STUDIES: SENSITIVITY OF IGNITION PARAMETERS TO DIFFERENT PHYSICS ASSUMPTIONS AND MODELS

5.1 Impurities

The level of impurities affects both the 'minimum power to ignite' and the stready state burn because of impurity radiation and fuel dilution. The effect of varying the carbon or beryllium content of the plasma from zero up to several percent is shown in Fig. 8 for the ITER-EDA case with medium energy NBI. It can be seen that up to 7% Be or 3% carbon impurity can be tolerated and ignition maintained.

Alternatively, the situation can be cast in the form of an *ignition domain* for plasma density $<n_e>$ and Z_{eff}. The result is shown in Fig. 9 which shows that there is essentially no density window for ignition operation if Z_{eff} exceeds 1.9. The result is not strongly dependent on whether carbon or beryllium is the dominant impurity.

5.2 Helium ash accumulation

The curves in Fig. 9 do not extend down to $Z_{eff}=1$. This is caused by the accumulation of helium ash particles, which are produced by the fusion reactions. The ash produced in the centre of the plasma has to diffuse out of the core towards the edge. The code assumes that 1% of the particle flux coming out of the plasma (including helium) is pumped away, and that the pumped fraction

is replenished with fresh D-T fuel. In this way, the helium content increases over time and reaches a steady state value of ~11%.

It is worth emphasising at this point, that the R-L-W model is an L-mode model. The particle fluxes derived from this model are therefore high. If the plasma is in H-mode the particle flux will be much smaller and the ignition will quench due to helium poisoning, which was pointed out by Rebut [1,5] and is reproduced by our present work. H-mode operation will require a significantly larger pumped fraction than 1% to keep helium levels down.

Note that the L-mode helium level of ~11% is much lower than the ~20% quoted by Rebut and Boucher *et al.* [1,3,5,6]. The difference between the helium levels found by us and those by Rebut is most likely caused by the modelling of an *additional edge transport barrier* in X-point configuration, which is considered (Boucher [6]) to be the consequence of an increased shear near the X-point. We could easily reproduce the higher levels using this particular modelling, but considered the experimental evidence for such an L-mode transport barrier as too weak. Because helium accumulates after ignition, the helium levels do not affect the *minimum power to reach ignition,* which is the main thrust of this paper. The transport barrier itself decreases the minimum power required for ignition, but we do not consider L-mode confinement which is better than R-L-W in this paper.

5.3 Energy confinement

All simulations presented so far in this paper have assumed L-mode confinement using the R-L-W transport model. It is widely recognised that there is a general lack of alternative *local* transport models which translate into expressions for global confinement, which agree with scaling laws like ITER89-P [2]. To simulate a global scaling we have used the R-L-W model to derive local transport coefficients, but then have applied a continuously varying scaling factor in order to force the computed global confinement into agreement with that given by eg. ITER89-P. The same scaling factor was applied over the entire plasma cross-section. Hence the simulation now effectively has R-L-W local scaling, but globally that of ITER89-P.

5.3.1. The optimism of Rebut-Lallia-Watkins scaling

R-L-W scaling is characterised by an offset linear form of confinement degradation. It features a so-called 'incremental confinement time', which does not decrease with power. Because the confinement degradation saturates with high power, R-L-W is inherently more optimistic than scaling laws like ITER89-P, where $\tau_E \sim P^{-0.5}$. Thus once the plasma ignites, it gains a gradually increasing enhancement factor over such L-mode scalings until at high values of P_α, the R-L-W plasma has an effective enhancement in the global energy confinement over ITER89-P of $\tau_E^{RLW}/\tau_E^{ITER89P} \sim 2$. Such an effect is favourable for ignition, because it increases the fusion product $n\tau_E T_i$ over time with the increasing alpha particle power. A time history of an igniting R-L-W plasma is shown in Fig. 10.

5.3.2 The pessimism of ITER89-P

The code was also run in such a way that the global confinement time (including fast particles) was equal to the ITER89-P scaling law. In this case the ITER89-P plasma will not even ignite at very high powers of NBI. Q~5 operation can be obtained at low Z_{eff} (Z_{eff}~1.3), but the case with 2% Be and 200 MW of 600 keV D^0 shown in Fig. 11 fails even to make this modest goal. Therefore it appears that ITER-EDA still requires optimistic assumptions about energy confinement to ignite in L-mode.

5.3.3. The difficulty of handling the H-mode threshold.

To avoid reliance on the R-L-W model, ITER-EDA must be designed for H-mode operation. This raises the question of the value for the H-mode power threshold.

The threshold power to achieve the H-mode is currently being investigated in a multi-machine H-mode power threshold database exercise. Preliminary results from the H-mode database working group [14] indicate that the power threshold can be scaled approximately as $n_e B_T S$, where n_e is the line averaged density, B_T is the toroidal field and S is the surface area of the plasma. The *coefficient* involved in the scaling depends on the database considered. The H-mode database working group [14] found:

$$P_{th} = 0.0089\ n_e\ B_T\ S \qquad [MW,\ 10^{19}m^{-3},\ T,\ m^2] \qquad (1)$$

whilst a fit by Ryter [15] to the data of the ASDEX-Upgrade tokamak indicates:

$$P_{th} = 0.0044\, n_e\, B_T\, S \qquad [MW,\ 10^{19}m^{-3},\ T,\ m^2] \qquad (2)$$

This fit by Ryter is consistent with consideration of the threshold data for 3 machines with constant elongation (k=1.6) and aspect ratio (R/a~3) viz: JFT-2M, DIII-D and JET. A fit by Thomsen [16] to the data from these 3 tokamaks gives the relation:

$$P_{th} = 0.004\, n_e\, B_T\, S \qquad [MW,\ 10^{19}m^{-3},\ T,\ m^2] \qquad (3)$$

A note of caution in using all these expressions is that at JET little evidence of a density dependence was seen (D. Campbell [17]).

ITER-EDA has a surface area of 1140 m^2. If one attempts to enter the H-mode at $n_e=5.10^{19}$ m^{-3}, the required power (additional plus alpha particles) would be 300 MW according to formula (1) and 140 MW according to formula (3).

If ITER-EDA would exhibit R-L-W confinement, there is no problem. Fig. 10 shows that the required power is easily achieved via the α-particles in L-mode. Triggering the H-mode would, however, be inconvenient in such a scheme because of the associated surge in fusion power and subsequent helium poisoning problems.

If ITER-EDA would exhibit ITER89-P energy confinement, one would expect that the α-particles produce roughly half as much power as the NBI system (Fig. 11). Formula (1) would therefore require 200 MW of beam power to achieve the H-mode, whereas Formula (3) would still require 100 MW beam power, which is significantly in excess of the presently foreseen 50 MW of installed additional power on ITER-EDA [18].

From the considerations given above, it is evident that it is hard to achieve an H-mode in ITER-EDA, assuming ITER89-P transport. However, if *enhanced L-mode confinement* is possible (and most tokamaks have reported cases of this), the α-particle power would be boosted and the required beam power is much reduced. Studying such schemes, however, is beyond the scope of this work.

5.3.4. H-mode operation

Once the H-mode is achieved in the ITER-EDA simulation there is no problem with ignition. The ignition threshold for H-modes is well below the H-mode threshold itself. Problems occur due to the much reduced particle transport in H-mode which causes more helium to accumulate.

Fig. 12 gives an example with 120 MW of Neutral Beam power into an ITER89-P plasma. After the H-mode is triggered, the energy confinement goes up to 2xITER89-P. As a consequence, the plasma ignites. After the beams are switched off the plasma remains ignited until the α-particle power is reduced (due to helium accumulation) below the H-mode threshold. Due to the collapse after the L-mode transition, the density limit (as adopted by the ITER-CDA team [2]) is exceeded and the plasma terminates. In achieving this simulation, the particle flux at the edge of the plasma was reduced by only 25% and the pumped fraction was 1%.

5.4 Sawteeth

The sawtooth model in PRETOR is described by Boucher [6]. To gauge the influence of sawteeth, the frequency (which depends on the fast particle content, including α's) was changed in the standard simulation. The period was varied from 0 to 25 seconds, and also a sawtooth-free case was simulated. Because of the current-density evolution, the mixing radius cannot be kept constant when the sawtooth period changes. As a result of this effect, the minimum power to ignite is not sensitive to the sawtooth period: it varies by only 10%.

The minimum power to ignite is strongly reduced for the sawtooth free case. The reduction is very sensitive to the minimum safety factor q_0 allowed to develop in the centre. For q_0=0.8 the reduction is 50%, for q_0=0.9 the reduction is 25%. The strong sensitivity is caused by the $q^2/\nabla q$ factor in the R-L-W model.

5.5 Anomalous fast particle losses

Two sources of anomalous fast particle losses may give rise to alterations in the power required to reach ignition. These occur from fishbone like instabilities or the excitation of Toroidal Alfven Eigenmodes (TAE modes). Fast beam particles and α-particles play a role in generating the instabilities, and are affected by them.

The fishbone mechanism is known to be more efficient at expelling particles which have become *deeply trapped* (White [19]). The population of such beam particles rises steeply with the approach to *perpendicular* (R_T=0) injection. For the JET-like injection geometry (R_T=4m) we expect trapped particles to occur in the ITER plasma at r/a≥0.65. Fig. 5 shows that for 600 keV D^o beams just over 40% of the beam particles are born outside r/a=0.65, the majority of these on the outboard side in trapped orbits. These particles may be subject to fishbone instabilities at high enough values of poloidal and fast particle β's. The fact that such instabilities have not been observed with any serious detrimental effect on JET indicates that for such geometries the fishbone instability can probably be safely ignored. The case of perpendicular injection would have to be more carefully assessed, however.

The avoidance of TAE modes requires that the *parallel* velocity of the passing fast ions should be either much smaller or much larger than the Alfven velocity (Cheng [20]). The parallel velocity of 600 keV D^o ions (injected at R_T=4m) is certainly well below the Alfven velocity. Problems can be expected for high energy beams (>1 MeV) injected at high tangency radius (>7m). The TAE modes should probably not be considered as a serious loss process for NBI particles on ITER, except perhaps for a system optimised for high energy current drive.

For α-particles, the birth velocity of 1.29 10^7 m/s could clearly lead to the creation of a population capable of exciting TAE modes, especially at high density. In order to evaluate the effects of such fast particle loss mechanisms, a prompt loss fraction f^{α}_{LOSS}, has been arbitrarily set in the α-heating code and varied. The increase in the minimum power to ignition (for a plasma following R-L-W transport) is shown in Fig. 13 as a function of f^{α}_{LOSS}. This graph assumes that the beam particles are not subject to an anomalous loss fraction f^{NBI}_{LOSS}. If they are, the minimum power to ignite is increased by a factor $1/(1-f^{NBI}_{LOSS})$.

5.6 Machine size

All global scaling laws show a strong positive advantage in increasing the size of the machine. The effect of machine size for R-L-W transport is shown in Fig. 14. Here, the minimum power to ignite the ITER-EDA [1], NET [21] and ITER-CDA [2] machines is plotted for a 600 keV D^o injection system with JET-like injection geometry ($R_T = R_0/2$, where R_0 is the major radius). The parameters of the 3 tokamak machines are given in Table 1.

The effect of a variable fraction of beryllium impurity is included. It can be seen that the ITER-CDA device will not sustain ignition (assuming R-L-W transport) for *any* NBI power if the Be content is 3%. ITER-EDA will tolerate up to 7% Be impurities. In going from ITER-EDA to ITER-CDA for a *pure plasma* the required NBI power to ignite is seen to increase by a factor ~4.

If, on the other hand,one considers ITER89-P confinement scaling (with a factor of 2 enhancement in the H-mode), the minimum power to ignite is 40% lower for ITER-CDA than for ITER-EDA due to a lower H-mode threshold (see sect. 5.3.3). This is due to the smaller size and lower toroidal field. The ignition domain for ITER-CDA will be much narrower, however.

6. BURN CONTROL

Many strategies for burn control of reactor plasmas are proposed in the literature and here we concentrate on two: *density control* and *additional power* control. Density control is the method favoured in discussions of the ITER-EDA (Rebut [1,5]). Neutral Beam Injection can play a role in additional power control and the two methods will be compared here.

In the simulations which follow, the plasmas are all assumed to follow R-L-W transport. The tokamak is ITER-EDA and the plasma simulated has 5% beryllium. Where NBI is used, 600 keV D^0 beams are simulated with a tangency radius of 4 metre. The only physics available to the feedback on fusion power is that fusion power increases with density or beam power.

6.1 Comparison between density and NBI burn control

Successful simulations of density burn control have been presented by Rebut *et al.* [5]. They showed that it is possible to control the output power of an ITER-EDA plasma (with 1% Be dilution) in the range P=200 - 800 MW. Below P=200 MW, density burn control was no longer possible and the ignition could no longer be sustained. The authors identified helium accumulation as the cause of this.

Their results can be readily understood if one considers the ITER-EDA (Z_{eff}, $\langle n_e \rangle$) *ignition domain* plotted in Fig. 9. The fusion power depends on the density and the minimum fusion power is given by the lower boundary of the ignition domain. The lower boundary at Z_{eff}=1.4 (which is 1% Be and accumulated He) is

close to the 10^{20} m^{-3} lower limit on the density which they achieve. If the density drops below the ignition boundary, ignition would be lost and the burn quenched, unless density control is fast enough to oscillate in and out of the ignition domain, thereby maintaining the desired power.

An example of such oscillation into and out of the ignition domain is given in Fig. 15. The beryllium concentration is 5% and therefore the ignition boundary is at higher density (Fig. 9). At *constant* (uncontrolled) density, the minimum P_α is 500 MW for $\langle n_e \rangle = 14.10^{19}$ m^{-3}. By oscillating the density into and out of the ignition domain it is possible to reduce the output power to 300 MW, but no lower. This result depends on the particle fluxes at the edge and the pumped fraction.

It is possible to extend the operational domain for density control by applying additional power to the plasma. Fig. 16 gives the output alpha particle power for a given density. Three curves, corresponding to 0, 40 and 60 MW of NBI are plotted. With the constant 40 MW power it is possible to obtain P=200 MW and with 60 MW of beam power it is possible to go much lower still. In fact, the lower ignition boundary in Fig. 9 has shifted towards a lower density if constant additional power is added to the power balance.

As density burn control obviously only works in or near the ignition domain, NBI burn control is considered for sub-ignited operation. NBI burn control fails in the ignition domain because it is impossible to couple negative power to the plasma. This is illustrated in Fig. 17(a), where the requested P=280 MW. The plasma density is ramped to 13.10^{19} m^{-3} under controlled NBI power. The plasma ignites around t=100 sec, and the power surges to 650 MW, uncontrolled. Helium ash accumulation subsequently quenches the burn and the NBI burn control maintains the power at 280 MW after this event. The surge in the beginning can be avoided entirely by first ramping the density to 12.10^{19} m^{-3} and later (t>180 sec, when the helium has accumulated) to 13.10^{19} m^{-3}, this is shown in Fig. 17(b). Power surges under NBI burn control are easier avoided further away from the ignition domain at lower fusion power.

Fig. 18 shows the required *time averaged neutral beam power* to obtain a certain P_α as a function of volume averaged density. Curves are plotted for 3 values of alpha particle power. They show that it is possible to obtain for the same density and beam power very different values of fusion power. The difference between

these points (where two curves intersect) is the ion temperature: In getting to these points the plasma has followed two different routes on the n_e-T_i diagram (an example of which is plotted in Fig. 1).

We conclude that NBI and density burn control are supplementary: NBI burn control works in the sub-ignited domain and density burn control in the ignited domain. NBI therefore is a useful tool to produce a wider range of plasmas, which will be useful both in the materials testing role of ITER, and also in the early 'Physics' phase, when the neutron yield will be required to be under tighter control to avoid excessive early irradiation of the device.

The sensitivity of NBI burn control to beam energy was tested with 1.3 MeV beam simulations. These beams have a longer slowing down time and heat the ions less (Fig. 4), which would make burn control more difficult. On the other hand, the beam penetration (Fig. 5) is much better. On balance, the 1.3 MeV beams offered a somewhat larger range in operating density than the 0.6 MeV beams.

6.2 Compatibility of burn control and ignition NBI systems.

It is clear from sect. 6.1 that the power requirement for ignition and burn control is quite similar; care had to be taken to avoid 'accidental ignition' (Fig. 17). The pulse length requirement for burn control is more stringent since long pulses are needed. For ignition only, the beam pulse can be stopped when the plasma is ignited. The conclusion is that a burn control NBI system is suitable for heating to ignition.

7. CURRENT DRIVE WITH NBI

A 1.3 MeV NBI system, optimised for current drive on ITER-CDA is described in the paper by the ITER-CDA team [2]. The NET team [21] describe a very similar system for current drive on NET. Recently, Mizuno *et al.* [22] published a conceptual design for a 2 MeV NBI system for the Steady State Tokamak Reactor SSTR. These systems all feature high energy and a tangential injection angle (close to the tokamak major radius) to optimise current drive efficiency.

Fig. 19 highlights the dependance of current drive efficiency (defined as $\gamma_{CD} = n_e R_0 I_{CD}/P_{CD}$; n_e is the line averaged density in 10^{20} m^{-3}, the driven current is in MA and the power in MW) on beam energy and tangency radius for ITER-EDA.

The current drive efficiency γ_{CD} is 0.4 for a reasonably optimised system. To drive 15 MA in an $n_e=10^{20}$ m^{-3} ITER-EDA plasma would require therefore some 300 MW of beam power, a fact already recognised by Rebut [1].

The system considered here (0.4-1.0 MeV D^o, R_T=4m) is not optimised for current drive. Its current drive efficiency γ_{CD} is practically zero (Fig. 19). Therefore, its current drive capability is negligible.

8. CONCLUSIONS

In this paper the beam parameters for an NBI system for ITER-EDA, optimised for ignition and burn control, rather than current drive have been investigated. We have shown that this optimisation leads to much lower beam power and energy for such a system. Optimum parameters are:

- Tangency radius $R_T \sim 4$ m (Port access and particle trapping)
- 400 keV < E_{beam} < 1000 keV (Penetration and shinethrough)
- Beam power ~ 50 MW for R-L-W transport (depending on plasma impurity levels)
- Long pulse length (for burn control).

Sensitivity studies showed that the required beam power for ignition is very sensitive to the way the energy confinement time behaves. For Rebut-Lallia-Watkins transport, 50 MW is sufficient to ignite a plasma with as much as 5% beryllium (sect. 3). For ITER89-P scaling the required beam power is certainly in excess of the L-H mode power threshold, even though there is a wide margin of uncertainty in this threshold (sect. 5.3.3).

Also, the level of impurities in the plasma (sect. 5.1) and anomalous fast particle losses (sect. 5.5) affect the ignition threshold significantly. In contrast, the exact sawtooth period had not much influence on the results (sect. 5.4).

The minimum power to ignite ITER-EDA is only a slowly varying function of beam parameters, provided they are chosen near the optimum stated above. The beam energy dependence becomes steep below $E(D^o)$=300 keV. The tangency radius dependence becomes steep for R_T>6 m. Shinethrough becomes important for E>1 MeV.

Substantial savings in size and cost can be gained by abandoning the current drive optimisation and adopting an optimisation for ignition and burn control. A conceptual design for such a system, based on the physics described in this paper, is presented by Hemsworth [4].

ACKNOWLEDGEMENTS

The authors would like to thank D. Boucher (ITER San Diego) for making the code PRETOR available and explaining its details. The useful discussions with E. Thompson, K. Thomsen, T. Jones, A. Bickley, (JET), E. Speth (IPP Garching), T.Todd (AEA Culham), J. Pamela, V. Basiuk and R. Hemsworth (CEA Cadarache) are highly appreciated.

REFERENCES

[1] P-H. Rebut, D. Boucher, C. Gormezano, B.E. Keen and M.L. Watkins A Fusion Reactor: Continuous or Semi-continuous? Plasma Physics and Controlled Nuclear Fusion, 35A(1993)A3 *or* JET-P(92)65

[2] K. Tomabechi, J.R. Gilleland, Yu. A. Sokolov, R. Toschi and the ITER team, ITER Conceptual Design, Nuclear Fusion 31(1991)1135

[3] P-H. Rebut *et al.*, Reports for consideration by the ITER Technical Advisory Committee in their Third Meeting (TAC-3), 9-11 September 1993, at Naka, Japan.

[4] R.S.Hemsworth, F. Jequier, J. Pamela and A. Simonin, Conceptual Design of a Neutral Beam System for a Next Step Tokamak, to be published in Fusion Engineering and Design.

[5] P-H. Rebut, D. Boucher, D.J. Gambier, B.E. Keen and M.L. Watkins, The ITER Challenge, Proc. 17th Symp. on Fusion Technology, Rome (1992), Fusion Engineering and Design 22(1993)7 *or* JET-P(92)92.

[6] D. Boucher and P-H. Rebut, Predictive modelling and Simulation of Energy and Particle Transport in JET, (Proc.IAEA Technical Committee meeting on Advances in Simulation and Modeling of Thermonuclear Plasmas, Montreal, Canada, 1992), IAEA, Vienna (1993) 142.

[7] P-H. Rebut, P.P. Lallia and M.L. Watkins, The Critical Temperature Gradient Model of Plasma Transport: Applications to JET and Future Tokamaks.(Proc. 12th Int. Conf., Nice, France, 1988) Vol. 2, IAEA, Vienna (1989) 2209

[8] D. Boucher, P-H. Rebut and M.L. Watkins, A Model for Particle Transport in the JET Tokamak, Comptes Rendus de l'Academie des Sciences 315(II)(1992)273 *or* JET-P(92)23

[9] H.P. Summers, Atomic Data and Analysis Structure, User Manual, to be published as JET report.

[10] T.H. Stix, Heating of Toroidal Plasmas by Neutral Injection, Plasma Physics 14(1972)367

[11] N.A. Uckan and J. Sheffield, A Simple Procedure for Establishing Ignition Conditions in Tokamaks, ORNL Report ORNL/TM-9722 (1985)

[12] The ITER team, private communication.

[13] E. Thompson, D. Stork, H.P.L. de Esch and the JET Team, The use of Neutral Beam Heating to Produce High Performance Fusion Plasmas, Including the Injection of Tritium Beams into the Joint European Torus (JET) Physics of Fluids B5(1993)2468

[14] H-mode Database Working Group, An Examination of the ITER H-mode Power Threshold Database, 20th EPS Conf. on Contr. Fusion and Pl. Physics, Lisbon, 1993 Europhysics Conference Abstracts 17C I-15 The coefficient 0.0089 is not part of the published paper, but was on the poster.

[15] F. Ryter *et al.*, Ohmic H-mode and H-mode Power Threshold in ASDEX Upgrade, 20th EPS Conf. on Contr. Fusion and Pl. Physics, Lisbon, 1993 Europhysics Conference Abstracts 17C I-23

[16] K. Thomsen, private communication.

[17] D. Campbell, private communication.

[18] TAC Members and Experts, Report of TAC-3 Meeting (held from 9-11 September 1993 in Naka, Japan), recommendations.

[19] R.B. White, R.J. Goldston, K. McGuire, A.H. Boozer, D.A. Monticello, W. Park, Theory of Mode-induced Beam Particle Loss in Tokamaks, Physics of Fluids 26(1983)2958

[20] C.Z. Cheng *et al.*, Alpha Particle Effects on Global MHD Modes, and Alpha Particle Transport in Ignited Tokamaks, 13th Int. IAEA Conference on Plasma Physics and Controlled Fusion Research (Washington 1990), vol. 2, IAEA Vienna (1991), p. 209

[21] The NET team, NET, Next European Torus, Predesign Report, Fusion Engineering and Design 21(1993)1

[22] M. Mizuno *et al,* Conceptual Design of a 2 MeV Neutral Beam Injection System For the Steady State Tokamak Reactor, Fusion Engineering and Design 23(1993)49

Table 1: Parameters of Tokamaks under study

	ITER-EDA	NET	ITER-CDA
R_0(m)	7.75	7.3	6.0
a(m)	2.8	2.43	2.15
k	1.6	2.0	2.0
B_0(T)	6.0	5.2	4.85
I_p(MA)	25.0	25.0	22

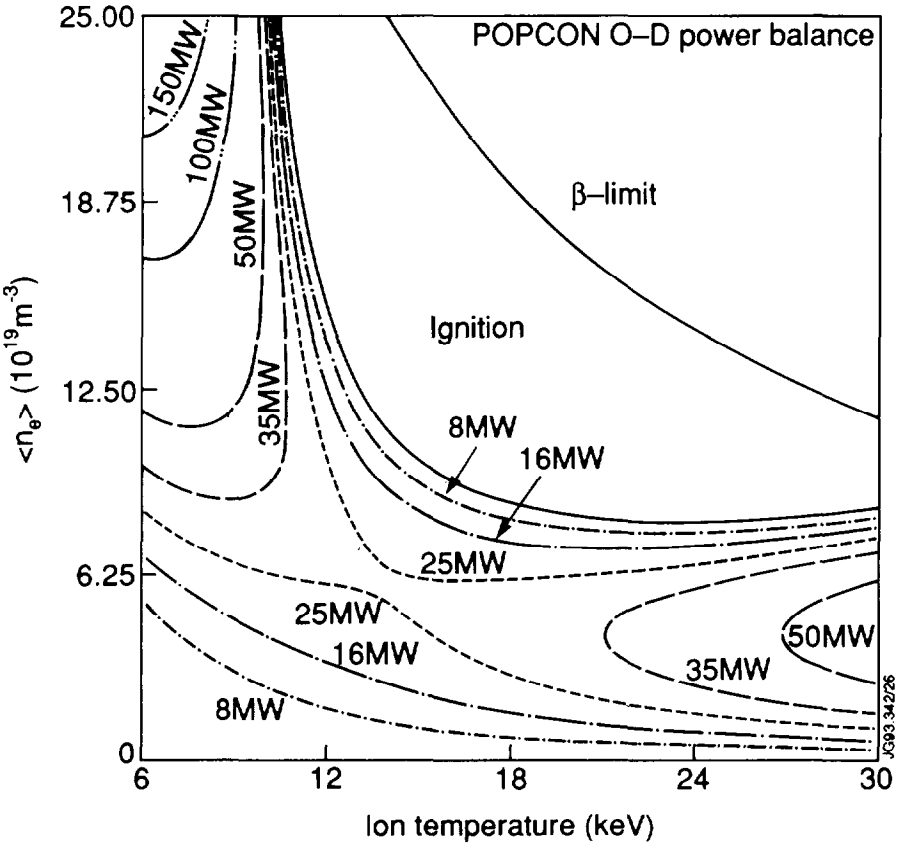

Fig.1: POPCON plot for ITER-EDA, R-L-W transport, showing contours of constant additional power.

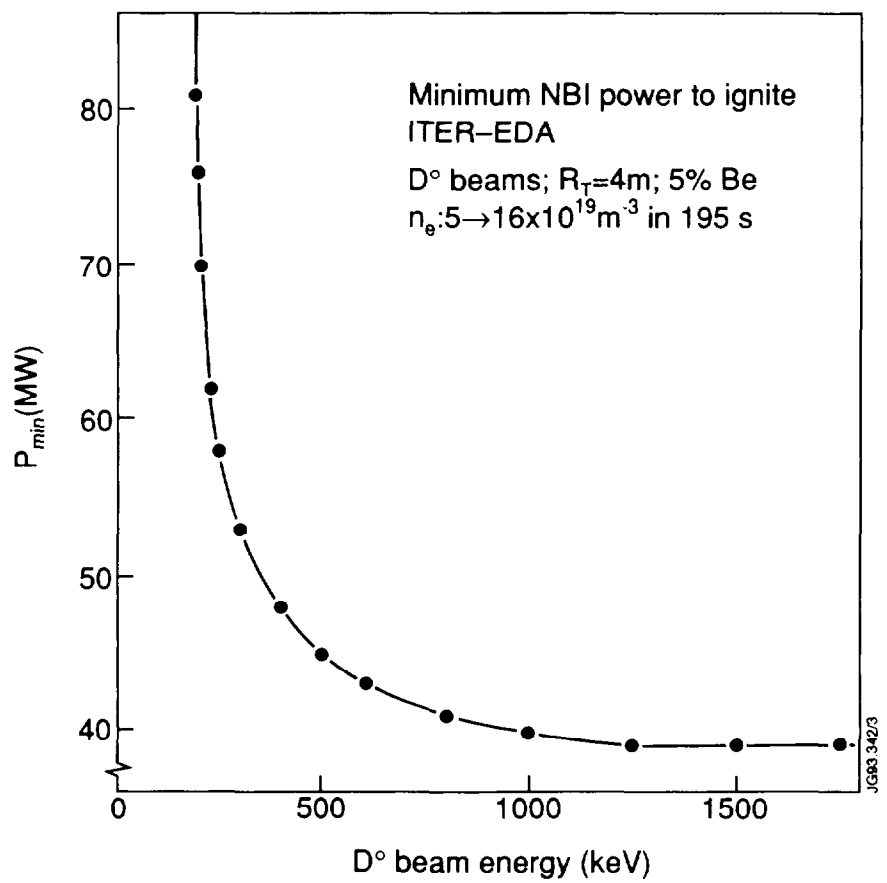

Fig.2: Minimum beam power to ignite ITER-EDA (5% Be).

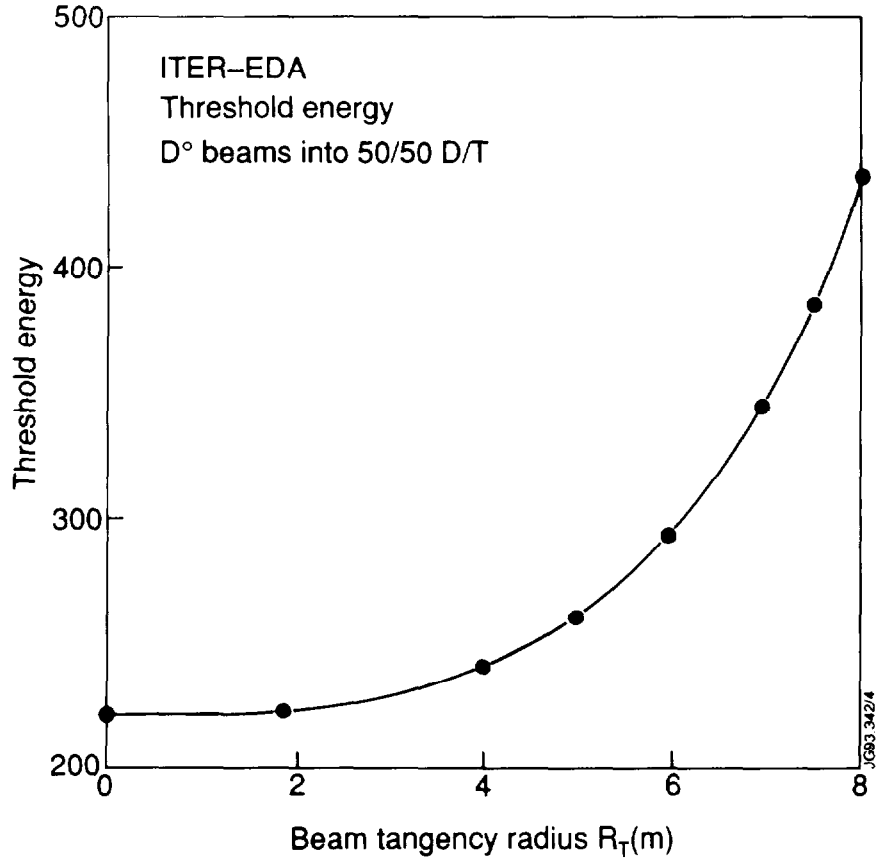

Fig.3: Beam Geometry dependence of the Threshold Energy (see text).

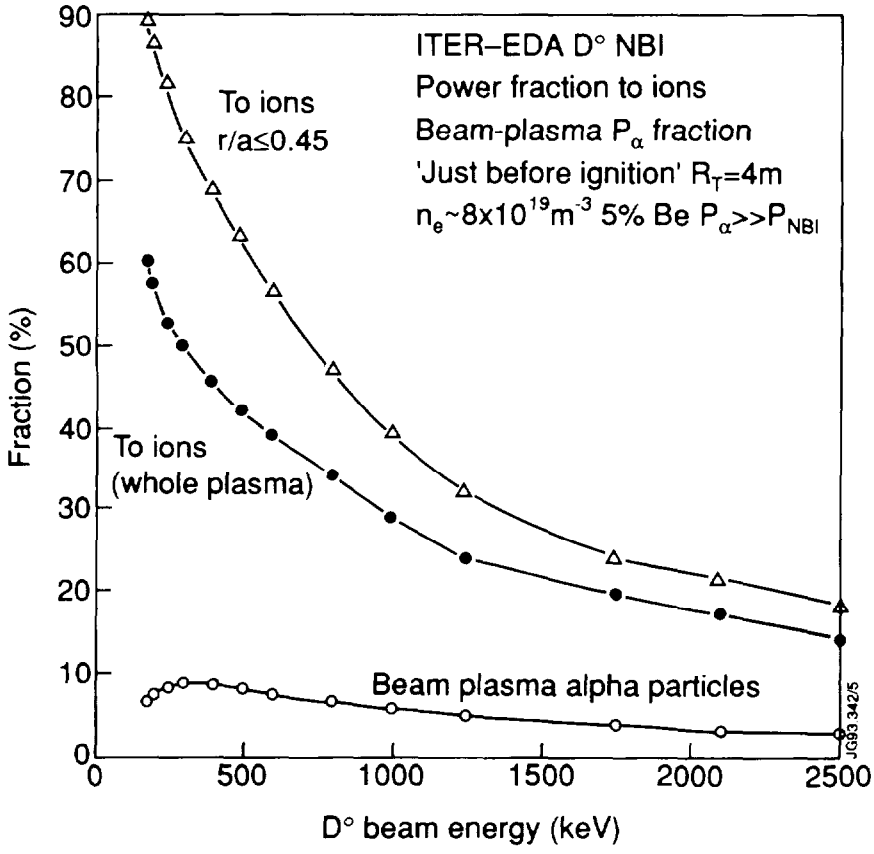

Fig.4: Beam power fraction coupled to the ions and beam-plasma alpha particle power fraction generated by the beams.

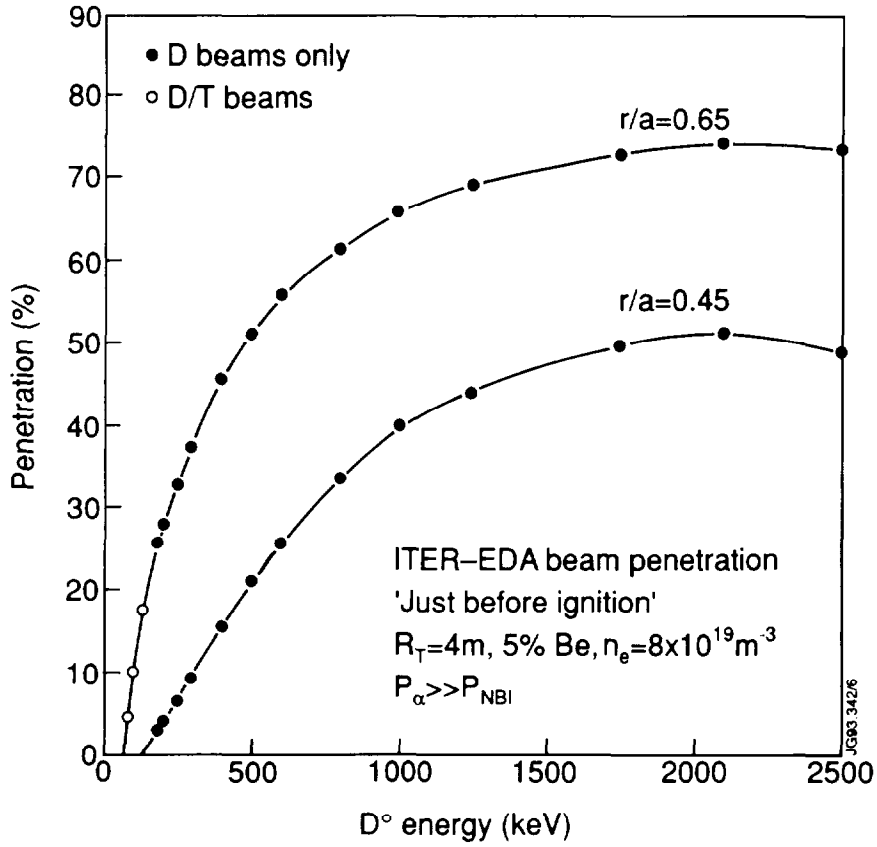

Fig.5: Beam penetration at n_e=8.10^{19} m^{-3}.

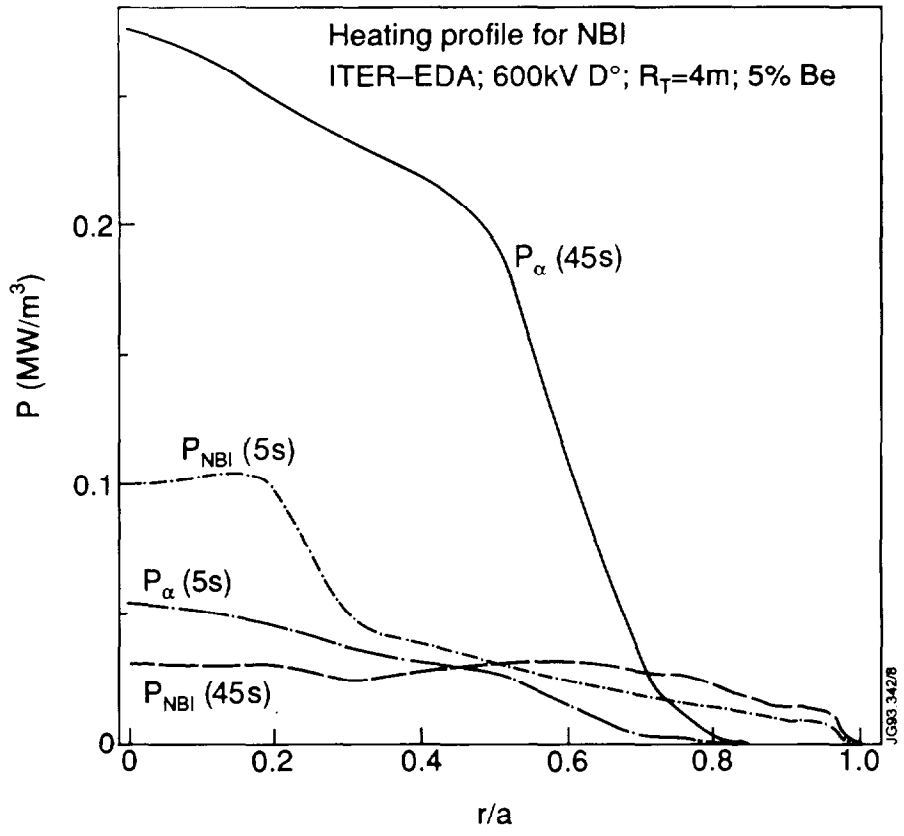

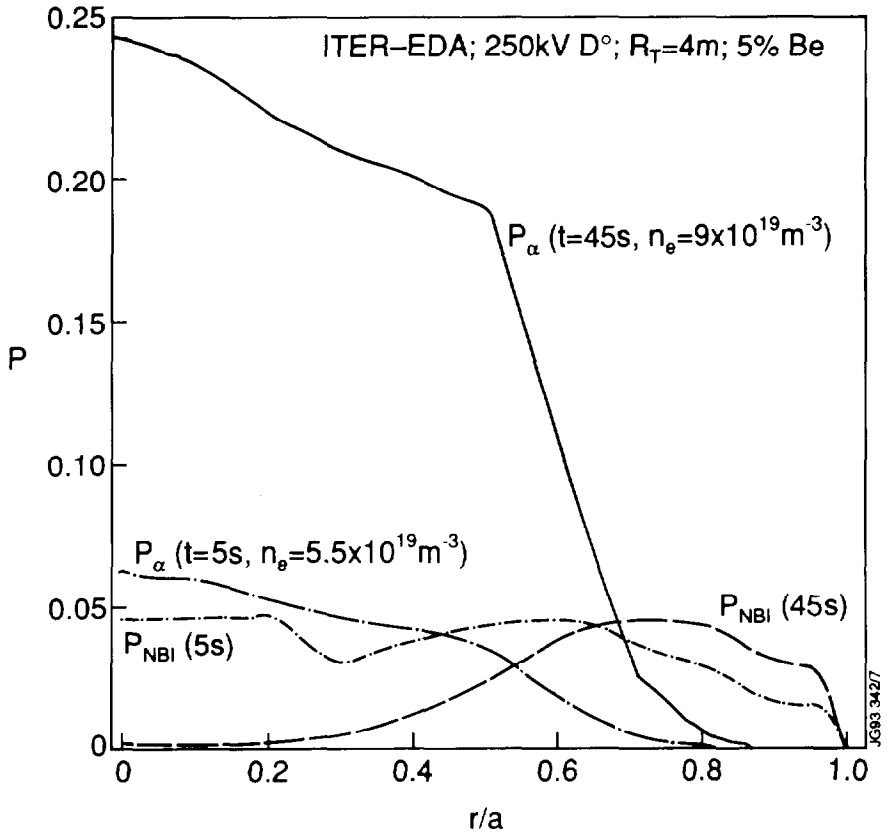

Fig.6: NBI and alpha particle heating profiles in ITER-EDA
(a) for 600 keV D^o
(b) for 250 keV D^o.

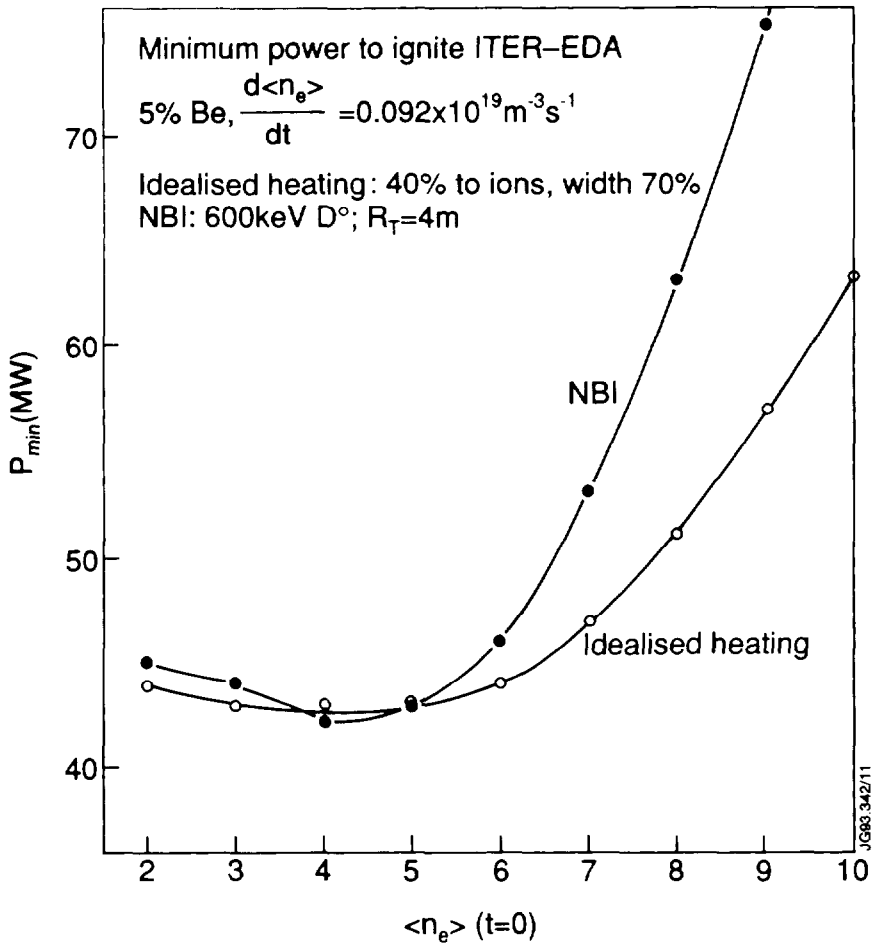

Fig.7: Minimum power to ignite ITER-EDA (5% Be) for 600 keV D^o NBI and for idealised heating with a constant deposition profile.

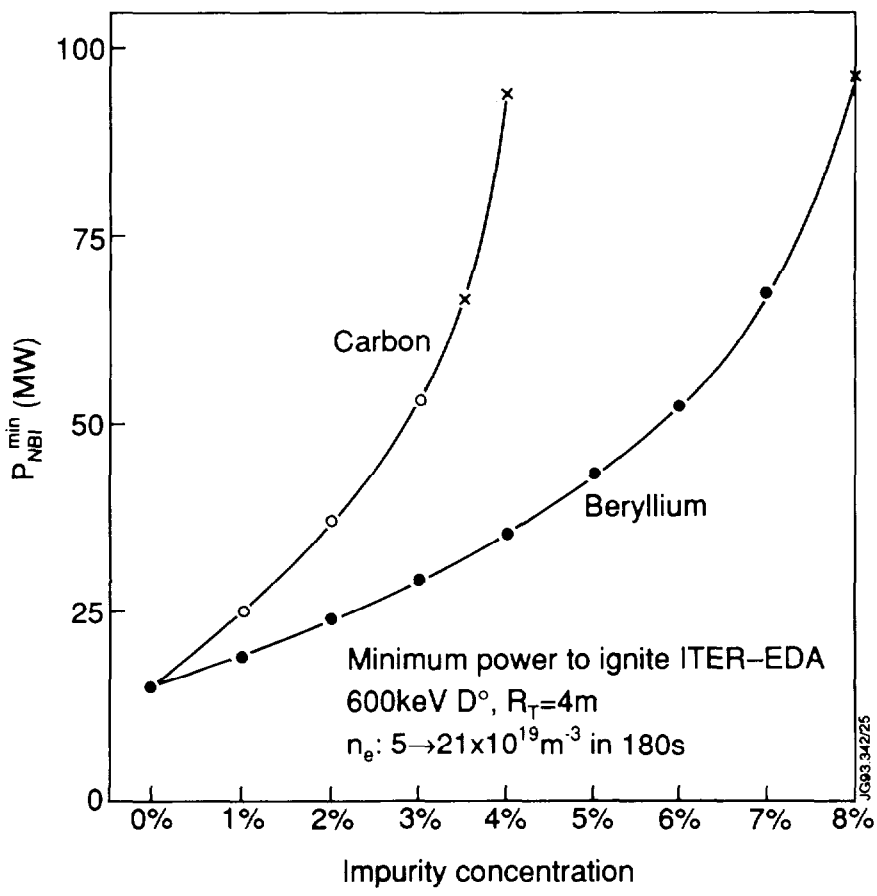

Fig.8: The effect of impurities on the NBI power required for ignition.

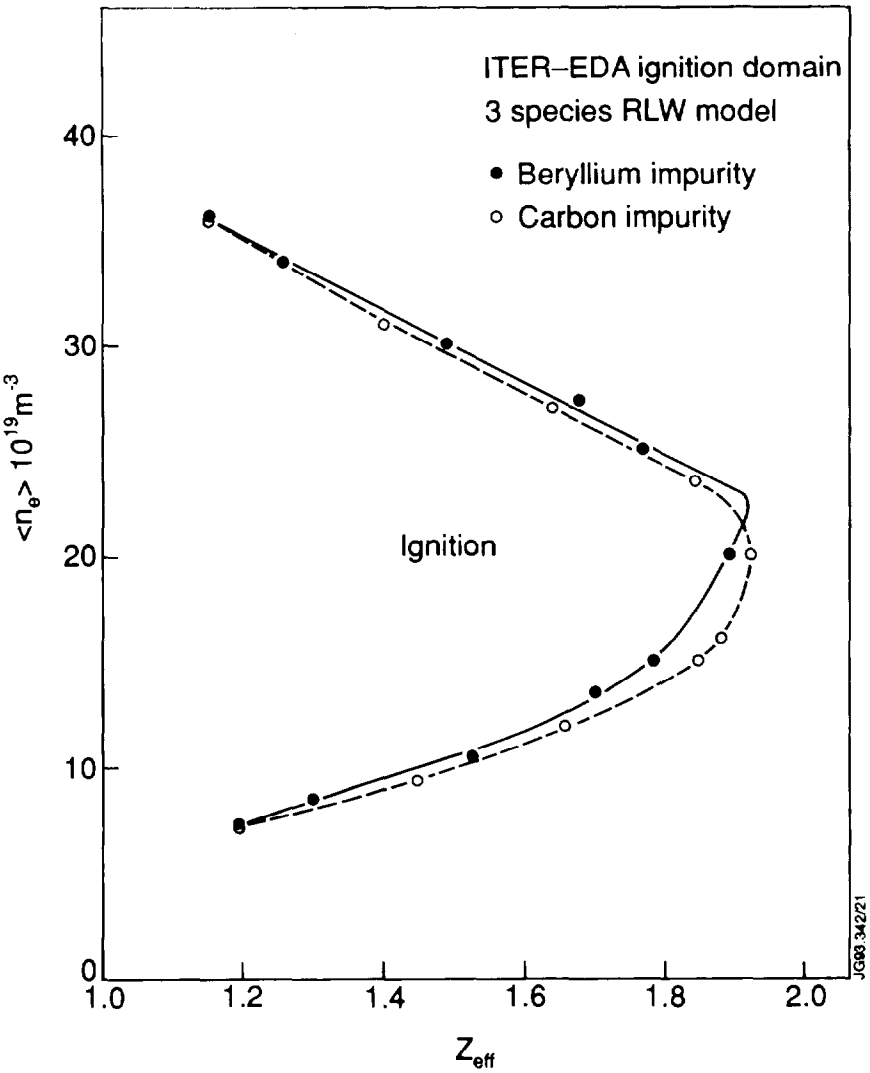

Fig.9: The ITER-EDA ignition domain for R-L-W transport.

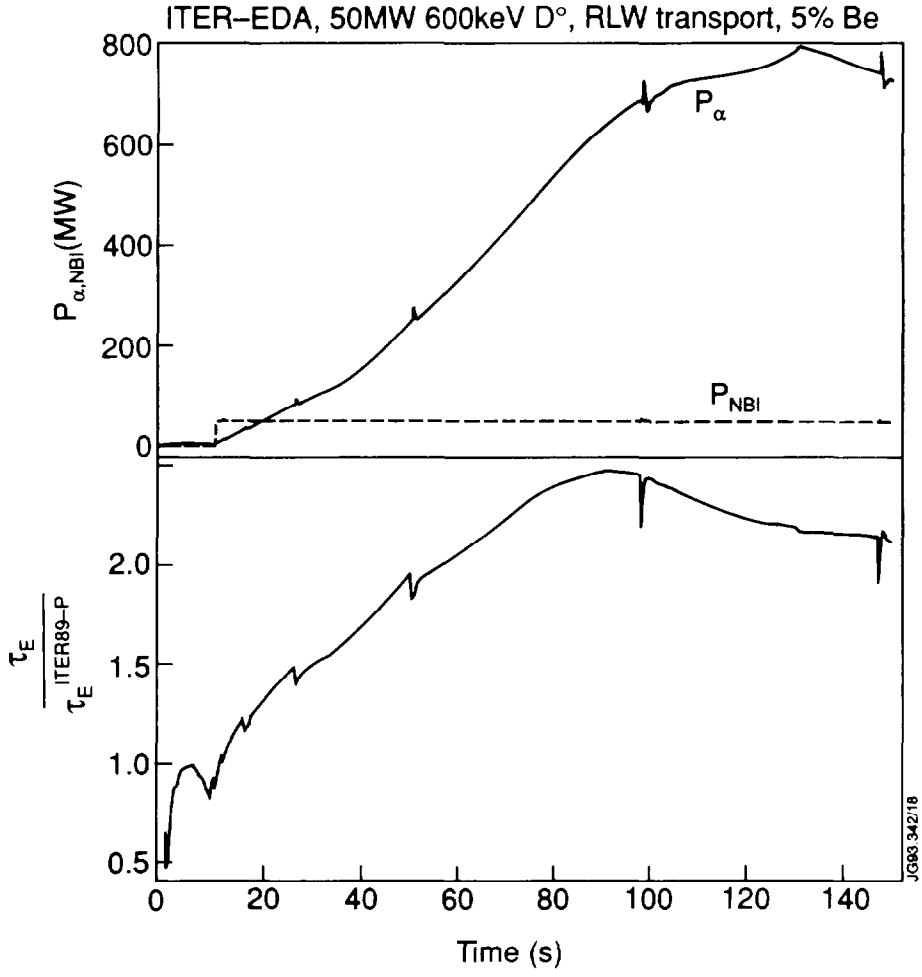

Fig.10: An igniting ITER-EDA plasma with R-L-W transport.
(a) Alpha particle power and NBI power
(b) R-L-W confinement enhancement relative to ITER89-P.

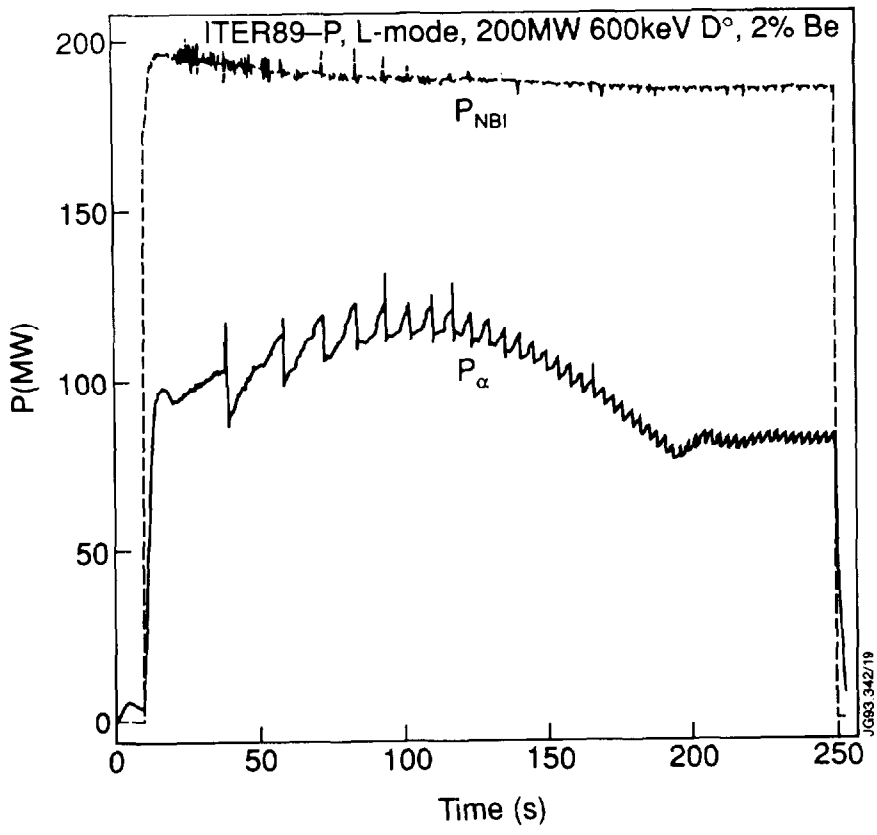

Fig.11: Alpha particle power and beam power for an ITER-EDA plasma with ITER89-P L-mode transport.

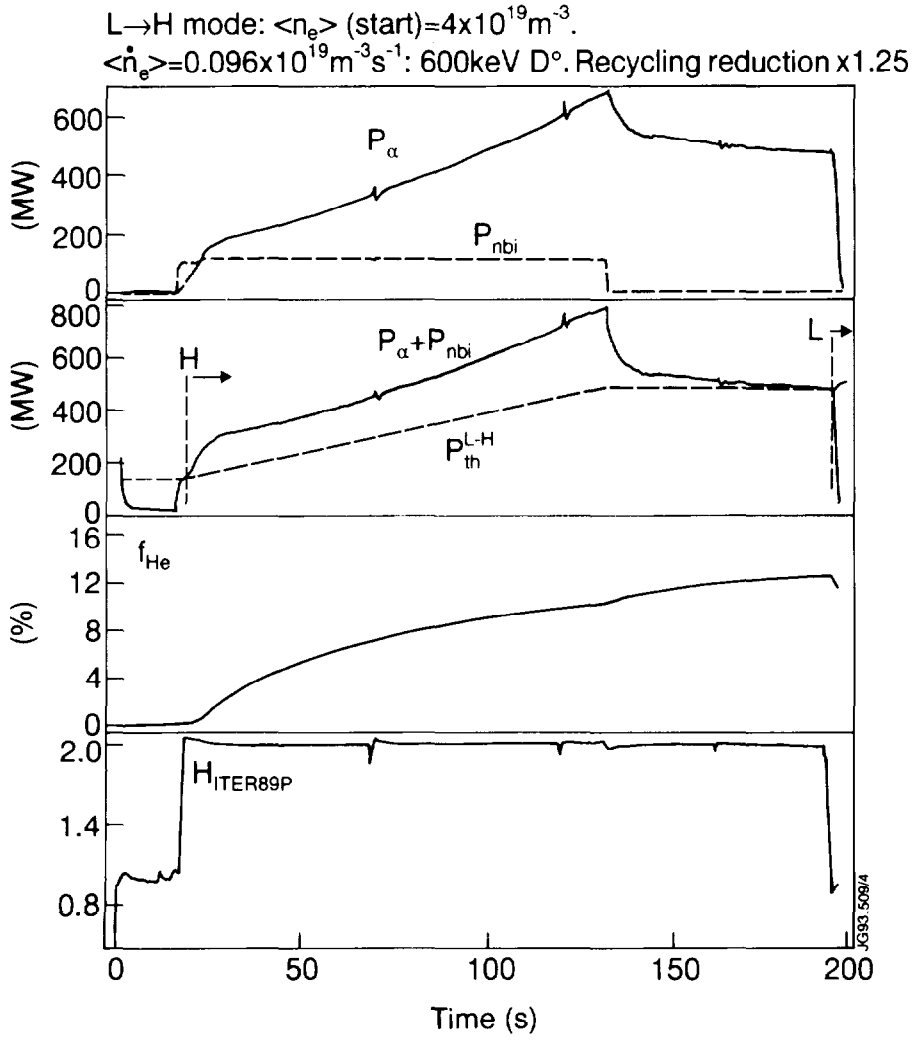

Fig.12: ITER89-P L-mode and H-mode simulation. The particle flux at the edge is reduced with only 20%.

(a) Alpha-particle power and beam power

(b) Total power coupled to plasma and the L-H threshold power (formula (3))

(c) Helium fraction in the plasma

(d) Energy confinement over ITER89-P global scaling

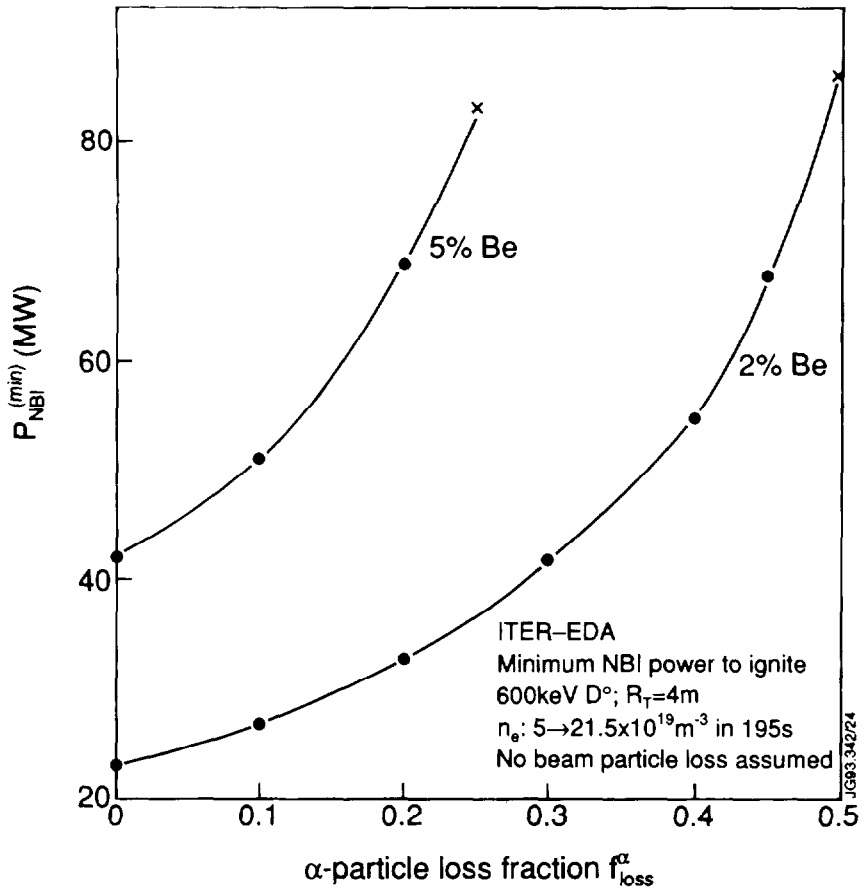

Fig.13: The dependence of the Minimum NBI power to ignite ITER-EDA on the prompt loss fraction of alpha particles.

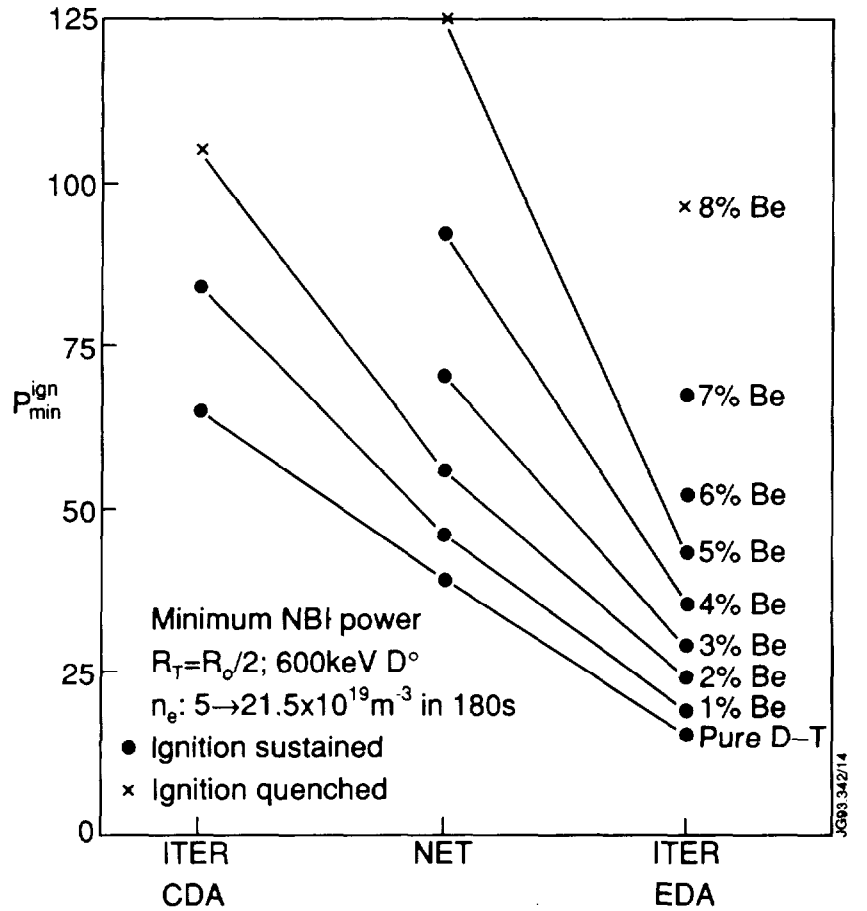

Fig.14: The Minimum NBI power required to ignite three tokamaks. Values for various impurity contration level are given.

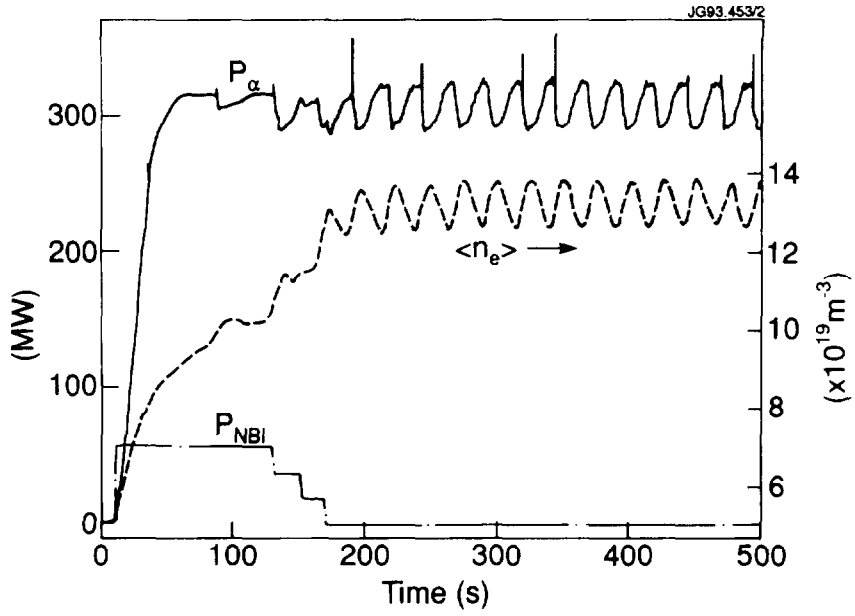

Fig.15: Density burn control near the ignition boundary. The sawtooth cycle enhances the density oscillations.

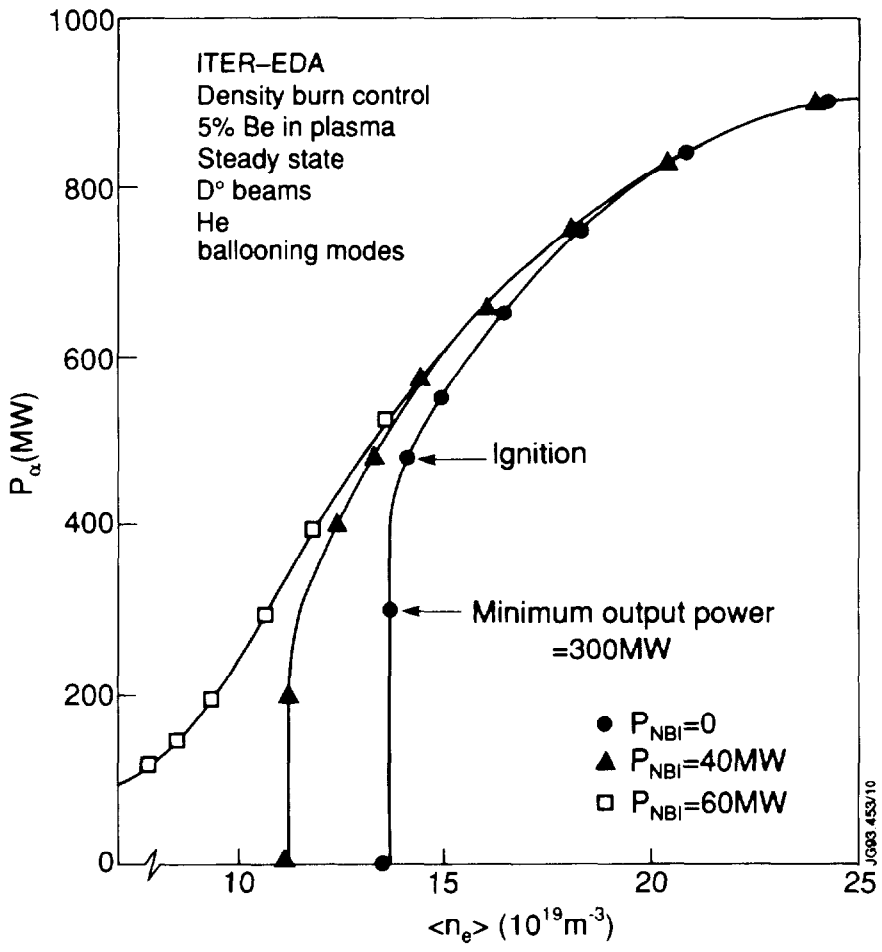

Fig.16: Operational domain for density burn control in ITER-EDA with 5% Be impurity. Curves for 0, 40 and 60 MW of additional beam power are given.

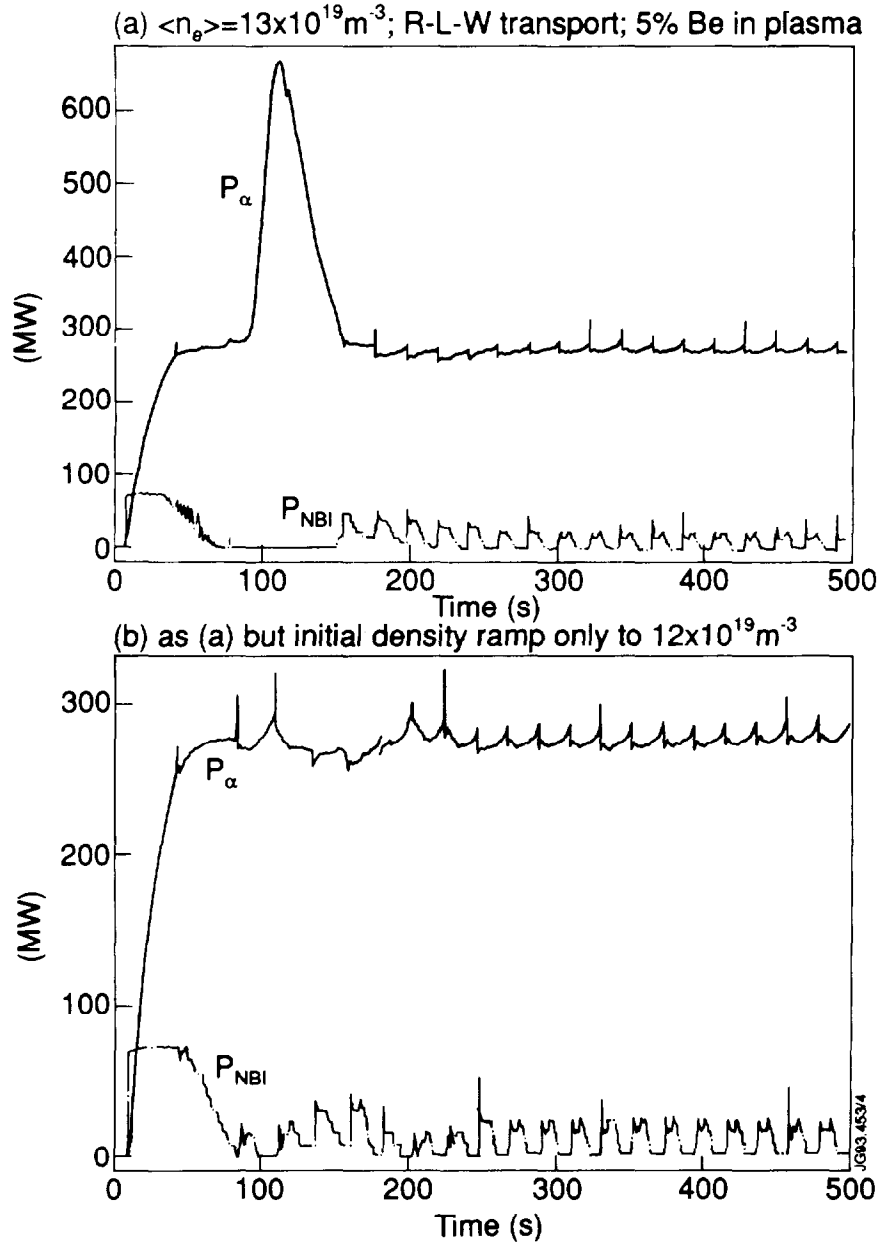

Fig.17: Burn control with NBI near the ignition domain.

(a) Fusion power excursion

(b) Avoiding the power excursion by slower density ramp

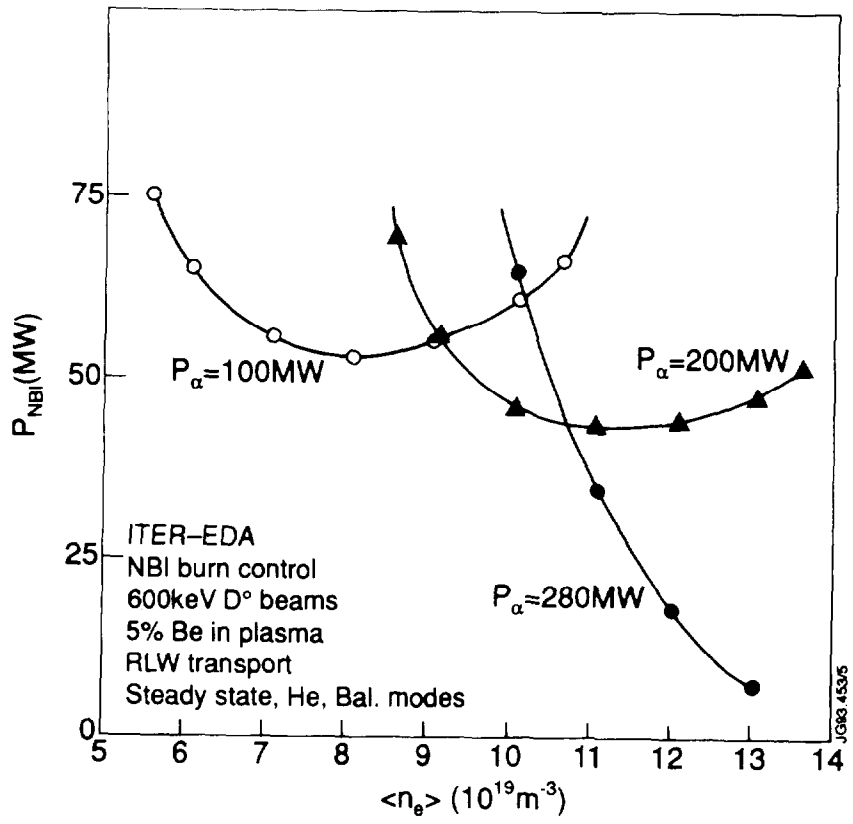

Fig.18: Operational domain for NBI burn control. Curves for three values of alpha particle power are given.

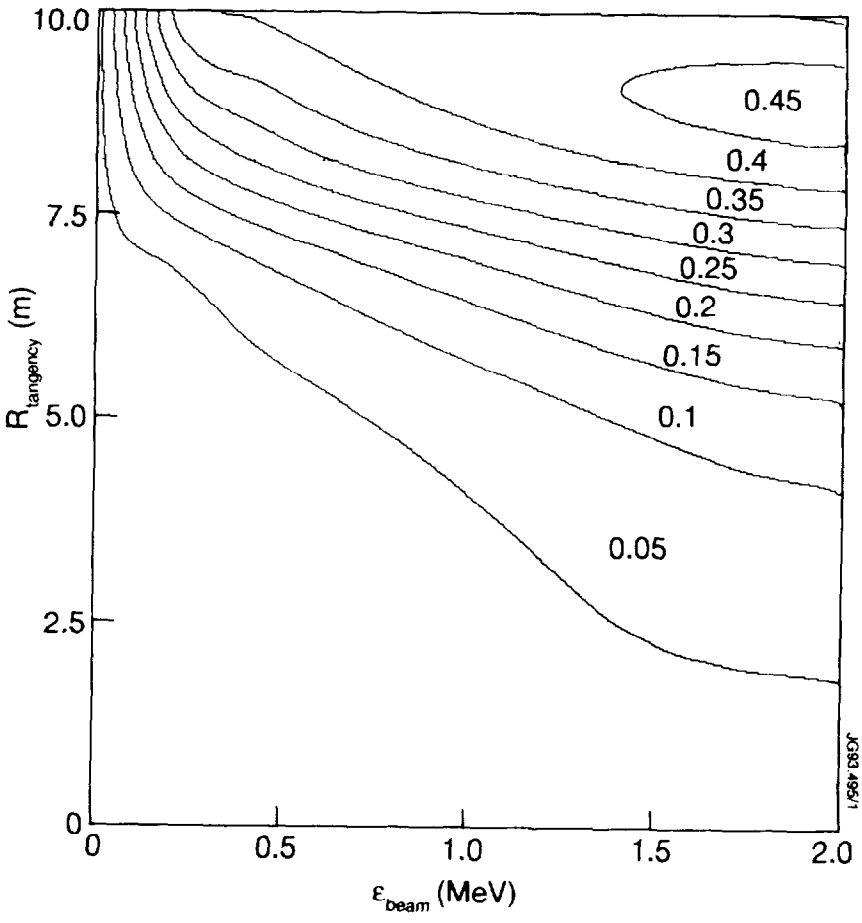

Fig.19: NBI current drive efficiency $_{CD}$ contours for ITER-EDA with the mid-point values shown for each region.